Effect of Particle size on Biomedical Behaviors of Sub-micron Silk Fibroin

Rou Li
Xuzhou Medical University
Xiao Li (lixiao_nm@smmu.edu.cn)
Changhai Hospital https://orcid.org/0000-0003-4135-2275
Ye Peng
Changhai Hospital
Dan ni Li
Changhai Hospital
Chao Cheng
Changhai Hospital
Guo rong Jia
Changhai Hospital
Chang jing Zuo
Changhai Hospital

Nano Express

Keywords: Silk fibroin, Particle size, Biomedical behaviors, Biological applications, Nuclear imaging

Posted Date: September 10th, 2020

DOI: https://doi.org/10.21203/rs.3.rs-74245/v1

Abstract

Due to the excellent physicochemical and biomedical properties, silk fibroin (SF) is a good source for the development of biomedical materials, where size selection of SF during biological application heavily affects the related biomedical behaviors. In this research, silk fibroin was step-wisely filtered and classified by syringe filter into four particle sizes ranges (< 200 nm, 200-450 nm, 450-800 nm and > 800 nm), and was then labeled with iodine-125 (^{125}I-SF) for nuclear imaging. Super early (0-40 minutes) and primary (1-72 hours) biodistribution of ^{125}I-SF were evaluated in Wistar rats. SEM-proved spherical or irregular silk fibroin powder with mixed size was not reuniting with each other in aqueous solution. For early *in vivo* distribution, four SF mostly gathered in the gastrointestinal tract (120-140 times to the background (accumulation in upper limb of left hind leg)), and a small amount (20-40 times) in bladder after injection within 40 min. For SF (< 200 nm, 200-450 nm and 450-800 nm) during the first 72 h, although there was decreasing trend over time, the gastrointestinal accumulation still accounted for the majority. Meanwhile, most of the SF in the bladder was expelled within 1 h and SF could be rarely seen in liver. Notably, SF (> 800 nm) almost gathered in the liver instead of the gastrointestinal tract after 10 h and got the peak value (280 times to the background) at around 48 h. The particle size directly determined the passive distribution of SF *in vivo*, which can not be ignored during drug design. Above all, these preliminary results may be referable for further biomedical application on silk fibroin.

Background

Silk fibroin (SF) extracted from silkworm cocoons is an easily available natural bio-polymer, which has a long history being used as surgical suture (1). As a natural protein, silk fibroin and its degradation products are non-toxic to cells and the body, and will not or rarely cause inflammation or immune rejection. Owing to its unique mechanical properties, diverse processability, good histocompatibility and controllable biodegradability, SF has been promoted as drug sustained-release carriers to control the delivery and release of drugs (2, 3), as tissue engineering materials such as bone tissue scaffolds (4), and as a wound healing dressing (5), etc. The practical application of silk fibroin is still being actively studied and developed, and has broad prospects in many fields.

Natural silk can be processed into various forms through a series of silk fiber processing, such as sponge, lyophilized powder, hydrogel and microspheres (6). Besides the morphology, the particle size is also an important factor affecting drug metabolism and application (7). For example, according to modifying the dendrimer size, ployamidoamine (PAMAM)-based gadolinium complex contrast agents will alter the route of excretion (8–10). Taking this feature, smaller sized contrast agents excreted through the kidney are suitable as functional renal contrast agents, while larger sized are found better suited for blood and lymphatic imaging. The similar phenomenon of size effect also exist in gold nanoparticles (11) and iron oxide (12). Like those nano and sub-micron materials, particle size of silk fibroin will potentially influence its blood clearance, metabolic pathways, and metabolic rate, especially when silk fibroin takes spherical shape in biomedical applications. Hence, finding out the corresponding size effect on biological behaviors is useful for effective and purposeful drug design.

So far, the biomedical applications of silk fibroin, especially as the drug carriers, were based on various size. For this non-ignorable issues, this research designs a systematic and visible research protocol that silk fibroin was labeled by iodine-125, so as to explore the size-dependent pattern of *in vivo* biological behavior via dynamic and timed single photon emission computed tomography (SPECT). Hopefully, it may provide a possible reference for selection of suitable size before biomedical application.

Methods

Filtration and classification of silk fibroin

Lyophilized silk fibroin powder (5 μm) was bought from Meilun Biotechnology Company. The purchased silk fibroin protein, which was processed by physical method after high pressure degumming, contained a mixture with particle size of 5 μm and below. Scanning electron microscope (SEM, S-4800, Hitachi company, Japan) was used to picture the surface morphology and structure of mixed silk fibroin. Accordingly, a certain amount of silk fibroin powder was suspended in water, then oscillated with ultrasound for 10 minutes. The obtained silk fibroin suspension was filtered by 0.8 μm, 0.45 μm, and 0.2 μm syringe filter one by one, to be separated in < 200 nm, 200-450 nm, 450-800 nm and > 800 nm sizes ranges, and abbreviated as SF_{200} to represent < 200 nm, $SF_{200\text{-}450}$ to represent 200-450 nm, $SF_{450\text{-}800}$ to represent 450-800 nm, SF_{800} to represent > 800 nm in the following (**Fig. 1A**).

Iodine-125 labeling of silk fibroin

1 mL silk fibroin suspensions that were adjusted to similar concentrations at 10 mg/mL, and 3.5 μL $Na^{125}I$ solution (10×10*7 Bq) were mixed in the reaction tube with iodogen catalyst. At room temperature, four kinds of ^{125}I-SF were obtained by reaction on the oscillator for 20 minutes. The radio-labeling rate was measured by thin-layer chromatography (TLC) using Whatman No.1 test paper at 1 h, 2 h, 4 h, 6 h, 12 h, 24 h, 48 h and 72 h, respectively and deionized water was used as a developing solvent (the R_f value of ^{125}I=1, R_f value of ^{125}I-SF=0).

In vivo Biodistribution

Animal care and all experimental procedures were performed under the approval of the Ethics Committee of Shanghai Changhai Hospital. *In vivo* biodistribution study was carried out on twelve adult Wistar rats (200 ± 10 g, 8-10 weeks, male), which were randomly divided into four groups (three rats for each group). Each of the four labeled silk fibroin was divided into three parts on average, then injected respectively (0.5 mL ^{125}I-SF, containing 8.3×10*6 Bq of ^{125}I) into four groups of rats via tail vein.

Immediately after injection, four groups of rats were scanned by SPECT/CT coherently in dynamic mode and followed by static mode at different time points. Specifically, in the early 10 minute, the whole body

images were collected every 30 seconds, and from 10 minute to 40 minutes, images were collected every 1 minute. Then all rats were scanned at 1 h, 3 h, 6 h, 10 h, 24 h, 48 h and 72 h, respectively.

Results And Discussion

Morphology and structure of SF

As shown in **Fig. 1B**, mixed size SF appeared as spheres or irregular lumps in aqueous solution not reuniting with each other. The SEM images showed abundant pores spreading on the surface of SF, which were in uneven distribution and size. The large number of pores were beneficial to the loading and release of drugs, as the structural basis of drug sustained-release carriers. Besides, I-125 labeled SF was at the origin of TLC, and free I-125 was not detected, which meet the requirements of SF tracer *in vivo* (**Fig. 1C**).

Early *in vivo* distribution (within 40 min)

^{125}I-SF began to diffuse to the whole body immediately after the injection through the tail vein, and the typical *in vivo* distribution of silk fibroin in the early 40 minutes was shown in **Fig. 2A**. It could be observed that the early distribution of silk fibroin with four sizes were similar. After injection through the blood, ^{125}I-SF gathered obviously in the gastrointestinal tract and excreted through urinary system. Meantime, there were no visible aggregation in other organs in the early time, such as the thyroid and liver, indicating good labeling stability and half-life of *in vivo* blood circulation of silk fibroin.

The curve of accumulation in ROI (region of interest) clearly demonstrated the change of ^{125}I-SF in each organ within the early 40 minutes (**Fig. 2B**), in which accumulation in upper limb of left hind leg serving as the background (the same below). Quantitative analysis results further verified the distribution of ^{125}I-SF in SPECT images. Obviously, most of the SF gathered in the gastrointestinal tract quickly after injection. The gastrointestinal uptake fluctuated at a high level (approximately 120-140 times to the background) during the 40 min. For bladder, the amount of aggregation showed a slow increasing trend and was 1/3-1/4 of the gastrointestinal tract. Meanwhile, the traced SF in liver kept at a low level (the amount was similar to that of the background) all the time. Both the qualitative and quantitative images suggested that gastrointestinal metabolism was the main pathway of silk fibroin super early metabolism.

Primary *in vivo* biodistribution (within 72 h)

The typical *in vivo* biodistribution of four ^{125}I-SF in the first 72 h was shown in **Fig. 3A**. In image of SF_{200}, the gastrointestinal tract was still the main organ where SF gathered. After 3 h, the amount of silk fibroin in the gastrointestinal tract decreased gradually, while there was rarely ^{125}I-SF in the bladder (**Fig. 3B (⊠)**). Only at 72 h, a little ^{125}I dissociated from the silk fibroin and gathered in the thyroid. Similarly, $SF_{200\text{-}450}$

mainly appeared in the gastrointestinal system and there was a decreasing trend after 10 h. Silk fibroin was still excreting through the urinary system at 24 h post injection (**Fig. 3B (Ⅹ)**). Meanwhile, almost no accumulation of ^{125}I were found in the thyroid until 72 h. Distribution image of $SF_{450-800}$ *in vivo* was roughly similar to that of $SF_{200-450}$ (**Fig. 3B (Ⅹ)**), but ^{125}I-SF gathered in the bladder until 48 h. In other words, the three kinds of SF shared a similar *in vivo* distribution and degradation process, however, the rate of intestinal deposition and clearance were significantly delayed by the increase of SF particle size. Besides, only a small amount of ^{125}I was detected in liver for these three size.

Totally different with the other three particle sizes, SF_{800} distributed almost in the liver after 10 h and maintained until 72 h, instead of gastrointestinal system (**Fig. 3B (Ⅹ)**). Traced with ^{125}I, the whole liver was fully displayed, which indicated a large amount of ^{125}I-SF was uptaken by the liver. Besides, thyroid was faintly visualized after 48 h. Taking the characteristics of liver deposition, SF_{800} can be designed as functional materials, such as embolic agents of hepatic artery. More detailed dynamic and timed SPECT images were shown in **Fig. S1**.

Quantitative images more vividly showed the change of silk fibroin in ROI, **Fig. 3C** presented ratio of ^{125}I-SF in organs of interest to background within 72 h. For SF_{200}, $SF_{200-450}$ and $SF_{450-800}$, the ratio in the gastrointestinal tract were highest and the peak could reached around 140. The bladder had a downward trend from about 10-20 times, while the liver remained a low level of no more than 10 times. In contrast to the other three sizes, the ratio of SF_{800} in gastrointestinal tract was obviously lower (the peak was close to 50 times). However, the curve of liver appeared a apparent upward trend at 10 h post-injection and arrived the peak (about 280 times) at around 48 h, while was only about 2-3 times before 10 h. Though there was a downward trend, the liver uptake still maintained a high ratio until 72 h.

Deiodization occurred at about 72 hours, and the distribution of silk fibroin could not be truly reflected after 72 hours, so the images were collected only until 72 h. According to the image of distribution within the first 72 h above, smaller sized silk fibroin (SF_{200}, $SF_{200-450}$, $SF_{450-800}$) had basically consistent metabolic pathway, when larger sized (SF_{800}) possessed its own characteristics. SF firstly entered the gastrointestinal tract for digestion and absorption, that was consistent with the metabolic pathway of exogenous protein in the body. Under the action of various protein digestive enzymes, it was decomposed into peptides and a small amount of amino acids. Additionally, most of the SF metabolized by the urinary system was excreted at the early stage, and SF could be observed in the bladder at only a few time points after 1 hour. Among the four sizes of silk fibroin, only the SF_{800} went into the liver within 72 h probably for further metabolism. Like most proteins in the body, silk fibroin need to be metabolized by the liver in order to reduce toxicity or further exert biological functions. The reason why SF with smaller sizes were not shown to enter the liver may be that small-sized proteins were easier to be excreted directly by the blood circulation and urinary system. Above all, this size effect were mainly reflected by differences on the rule of *in vivo* biodistribution and metabolism, which was conducive to guide drug design. Taking the SF_{800} as example, it is suitable to serve as a material that needs to stay in the liver for a long time.

Conclusion

Particle size, as important factor in drug application, also directly affects the biological behavior of silk fibroin. Silk fibroin with different particle sizes have their own characteristics. The metabolic pathway of silk fibroin with the particle size less than 800 is similar, mainly intestinal metabolism, and the size influences the deposition rate and degradation rate. While silk fibroin with size larger than 800 is metabolized in the gastrointestinal tract in the early stage, and mainly in the liver after 10 hours. Hence, size-dependent biodistribution and metabolism should be overall considered before potential research and clinical design of silk fibroin.

Abbreviations

SF: Silk fibroin; SEM: Scanning electron microscopy; SPECT: Single photon emission computed tomography; ROI: Region of interest.

Declarations

Availability of data and materials

All data generated or analysed during this study are included in this published article [and its supplementary information files].

Competing Interests

The authors declare that they have no competing interests.

Authors' Contributions

RL drafted the manuscript. RL, YP and XL carried out the experiments. YP and CC did the data collections and statistics. DL and GJ were responsible for searching related literature. XL and CZ designed this research and made revisions. All authors read and approved the final manuscript.

Acknowledgements

Not applicable.

Funding

This work was funded by the National Natural Science Foundation of China (81471714, 81871390) and National Natural Science Foundation Youth Project (81701761).

References

1. Omenetto FG, Kaplan DL (2010) New opportunities for an ancient material. Science 329(5991):529–531
2. Kundu B, Rajkhowa R, Kundu SC, Wang XG (2013) Silk fibroin biomaterials for tissue regenerations. Adv Drug Deliv Rev 65:457–470
3. Gong H, Wang J, Zhang J, Wang X (2019) Control of octreotide release from silk fibroin microspheres. Mater Sci Eng C Mater Biol Appl 102:820–828
4. Gholipourmalekabadi M, Mozafari M, Bojnordi MN, Hashemi-Soteh MB, Salimi M, Rezaei N et al (2015) In vitro and in vivo evaluations of three-dimensional hydroxyapatite/silk fibroin nanocomposite scaffolds. Biotechnol Appl Biochem 62(4):441–450
5. Gholipourmalekabadi M, Sapru S, Samadikuchaksaraei A, Reis RL, Kaplan DL, Kundu SC. Silk fibroin for skin injury repair: Where do things stand? Adv Drug Deliv Rev. 2019;S0169-409 × (19)30164-4
6. Najberg M, Haji Mansor M, Taillé T, Alvarez-Lorenzo C (2020) Aerogel sponges of silk fibroin, hyaluronic acid and heparin for soft tissue engineering: Composition-properties relationship. Carbohydr Polym 237:116107
7. Li X, Hu Y, Xiao J, Cheng DF, Xiu Y, Shi HC (2015) Morphological effect of non-targeted biomolecule-modified MNPs on reticuloendothelial system. Nanoscale Res Lett 10:367
8. Sheikh S, Nasseri MA, Chahkandi M, Allahresani A, Reiser O (2020) Functionalized magnetic PAMAM dendrimer as an efficient nanocatalyst for a new synthetic strategy of xanthene pigments. J Hazard Mater 400:122985
9. Gao Y, Wang J, Chai M, Li X, Deng Y, Jin Q et al (2020) Size and charge adaptive clustered nanoparticles targeting the biofilm microenvironment for chronic lung infection management. ACS Nano 14(5):5686–5699
10. Wang B, Davis TP, Ke Puchun, Sun YX, Wu YH, Ding F (2018) Understanding effects of PAMAM dendrimer size and surface chemistry on serum protein binding with discrete molecular dynamics simulations. ACS Sustain Chem Eng 6(9):11704–11715
11. Engstrom AM, Faase RA, Marquart GW, Baio JE, Mackiewicz MR, Harper SL (2020) Size-dependent interactions of lipid-coated gold nanoparticles: Developing a better mechanistic understanding through model cell membranes and in vivo toxicity. Int J Nanomedicine 15:4091–4104
12. Yang L, Kuang HJ, Zhang WY, Aguilar ZP, Xiong YH, Lai WH (2015) Size dependent biodistribution and toxicokinetics of iron oxide magnetic nanoparticles in mice. Nanoscale 7(2):625–636

Figures

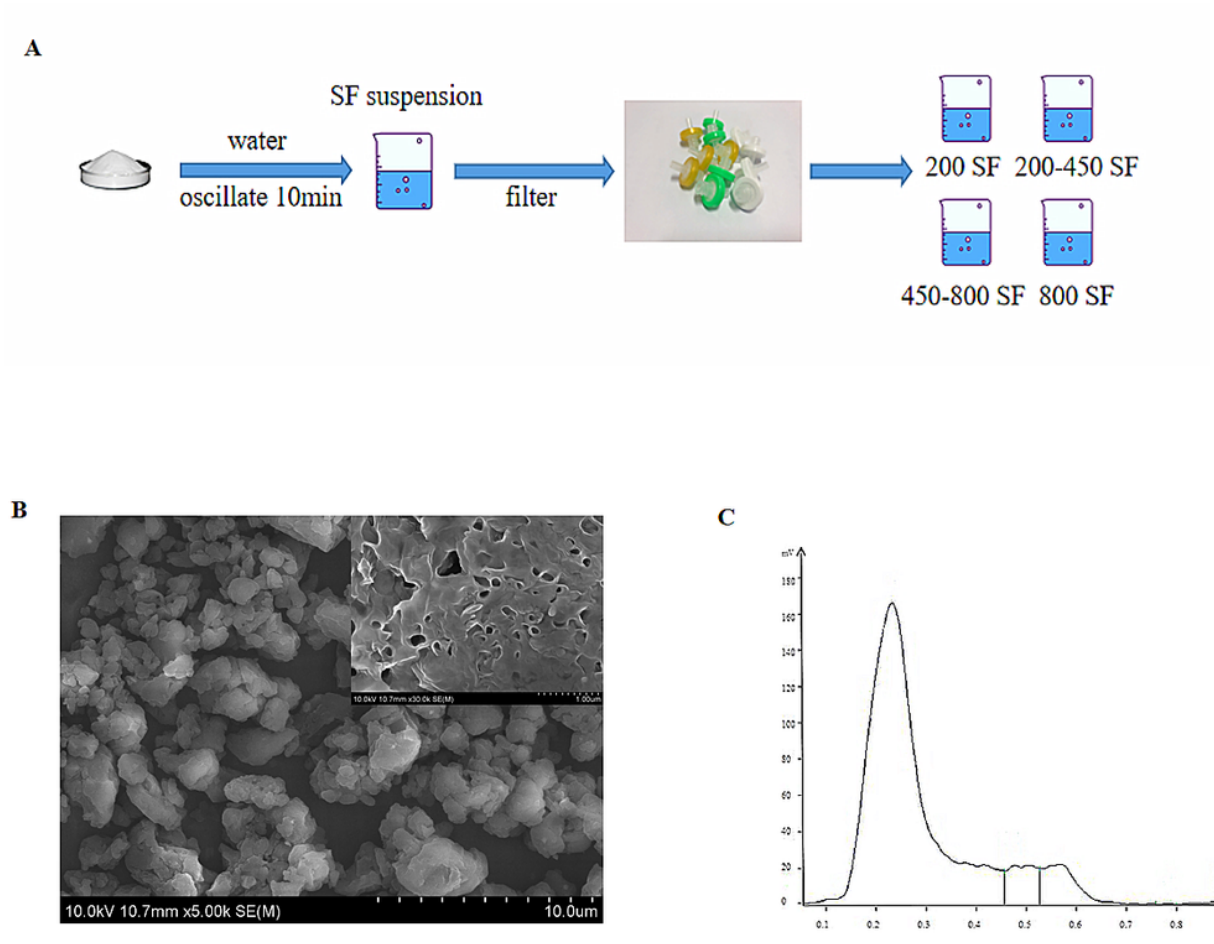

Figure 1

(A) Filtration and classification procedure of SF. (B) SEM of silk fibroin. Picture in the upper right corner was porous structure on the surface. (C) Radio-TLC spectrum of I-125 labeled SF.

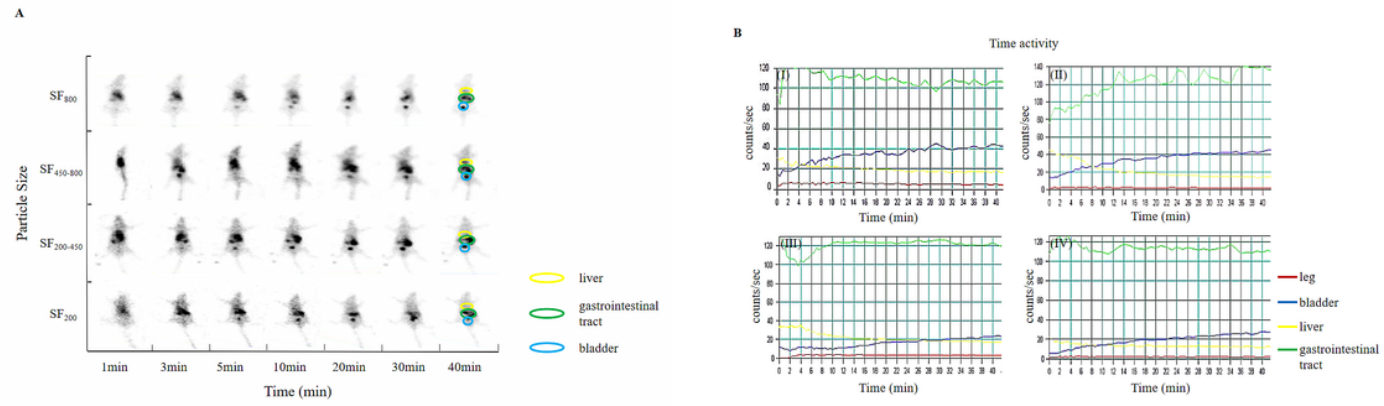

Figure 2

(A) SPECT images of rats after injecting 125I-SF via tail vein within 40 min. (B) The curve of 125I-SF in ROI within 40 min. (□) SF200, (□) SF200-450, (□) SF450-800, (□) SF800

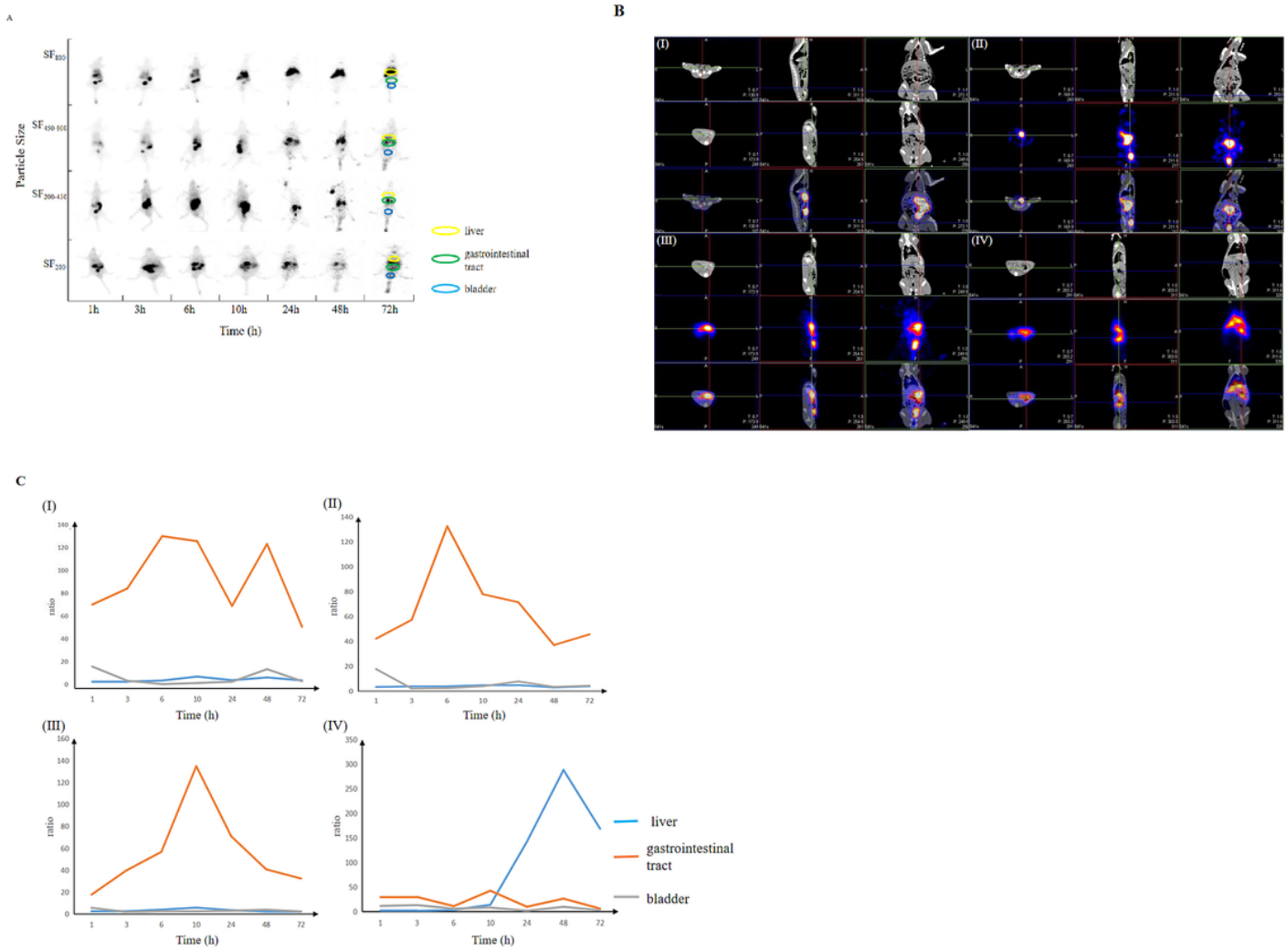

Figure 3

(A) SPECT images of rats after injecting 125I-SF via tail vein within 72 h. (B) SPECT/CT images of rats within 72 h. (□) SF200 (3 h), (□) SF200-450 (24 h), (□) SF450-800 (24 h), (□) SF800 (24 h). (C) The curve of the ratio of 125I-SF in ROI to the background within 72 h. (□) SF200, (□) SF200-450, (□) SF450-800, (□) SF800

Supplementary Files

This is a list of supplementary files associated with this preprint. Click to download.

- SF800.gif
- SF450800.gif

- SF200450.gif
- SF200.gif